Variational matrix-product-state approach to quantum impurity models

A. Weichselbaum,[1] F. Verstraete,[2] U. Schollwöck,[1] J. I. Cirac,[3] and Jan von Delft[1]
[1]*Physics Department, Arnold Sommerfeld Center for Theoretical Physics, and Center for NanoScience, Ludwig-Maximilians-Universität München, 80333 Munich, Germany*
[2]*Institut der Theoretischen Physik, Universität Wien, Boltzmanngasse 3, A-1090 Vienna, Austria*
[3]*Max-Planck-Institut für Quantenoptik, Hans-Kopfermann-Strasse 1, Garching D-85748, Germany*
(Received 25 August 2008; revised manuscript received 27 April 2009; published 13 October 2009)

We present a unified framework for renormalization group methods, including Wilson's numerical renormalization group (NRG), and White's density-matrix renormalization group (DMRG), within the language of matrix-product-states. This allows improvements over Wilson's NRG for quantum impurity models, as we illustrate for the one-channel Kondo model. Moreover, we use a variational method for evaluating Green's functions. The proposed method is more flexible in its description of spectral properties at finite frequencies, opening the way to time-dependent, out-of-equilibrium impurity problems. It also substantially improves computational efficiency for one-channel impurity problems, suggesting potentially *linear* scaling of complexity for n-channel problems.

DOI: 10.1103/PhysRevB.80.165117 PACS number(s): 72.15.Qm, 75.20.Hr, 02.70.−c, 78.20.Bh

Wilson's numerical renormalization group (NRG) is a key method[1] for solving quantum impurity models such as the Kondo, Anderson, or spin-boson models, in which a local degree of freedom, the "impurity," is coupled to a continuous bath of excitations. These models are of high relevance in the description of magnetic impurities, quantum dots, and problems of decoherence. NRG has been used with great success to calculate both thermodynamic[1,2] and dynamical[3–6] properties. It is, however, of limited use in more complex situations: computational cost grows exponentially for a coupling to multiple bands in the bath. In systems out-of-equilibrium or with time-dependent external parameters, such as occur in the tuning of quantum dots, difficulties arise due to NRG's focus on low-energy properties through its logarithmic discretization scheme which looses accuracy at high spectral frequencies.

In the present paper, we draw attention to the fact that states generated by the NRG have the structure of *matrix-product-states* (MPS)[7,8] on a one-dimensional geometry. This is a simple observation, which however has important conceptual and practical implications:

(i) As White's density-matrix renormalization group (DMRG)[9] for treating quantum chain models is in its single-site version identical to variational MPS,[8] NRG, and DMRG are now seen to have the same formal basis of matrix-product-states, resolving a long-standing question about the connection between both methods. (ii) *All* NRG results can be improved upon systematically by *variational optimization* in the space of variational matrix-product-states (VMPS) of the same structure as those used by NRG. This does not lead to major improvements at $\omega=0$ where NRG works very well, but leads to the inclusion of feedback from low-to-high-energy states, also allowing the relaxation of the logarithmic bath discretization of NRG: spectra away from $\omega=0$ can be described more accurately and with higher resolution. (iii) Recent algorithmic advances using VMPS,[8] in particular those treating time-dependent problems,[10,11] can now be exploited to tackle quantum impurity models involving time dependence or nonequilibrium; this includes applications to the description of driven qubits coupled to decohering baths, as relevant in the field of quantum computation. (iv) The VMPS algorithm allows ground state properties of quantum impurity models to be treated more efficiently than NRG: the same accuracy is reached in much smaller ansatz spaces (roughly of square-root size). Moreover, our results suggest that for many (if not all) n channel impurity problems it should be feasible to use an *unfolded* geometry, for which the complexity will only grow linearly with n.

The present paper provides a "proof of principle" for the VMPS approach to quantum impurity models by applying it to the one-channel Kondo model. We reproduce the NRG flow of the finite size spectrum,[2] and introduce a VMPS approach for calculating Green's functions, as we illustrate for the impurity spectral function,[3] which yields a significant improvement over existing alternative techniques.[12–15] Our results illustrate in which sense the VMPS approach is numerically more efficient than the NRG.

I. NRG GENERATES MATRIX-PRODUCT-STATES

To be specific, we consider Wilson's treatment of the Kondo model, describing a local spin-1/2 impurity in an external magnetic field B coupled to a fermionic bath. To achieve a separation of energy scales, the bath excitations are represented by a set of logarithmically spaced, discrete energies $\omega_n=\Lambda^{-n}$, where $\Lambda>1$ is a "discretization parameter."[1] By tridiagonalization, the model is then mapped onto the form of a semi-infinite chain $\mathcal{H}=\lim_{N\to\infty}\mathcal{H}^N$ where[1]

$$\mathcal{H}^N = BS_z - 2J\mathbf{s}\cdot\mathbf{S} + \sum_{n=1}^{N-1}\xi_n(c^\dagger_{n\mu}c_{n+1,\mu} + c^\dagger_{n+1,\mu}c_{n\mu}). \quad (1)$$

$\mathcal{H}^N$ describes an impurity spin $\mathbf{S}$ in a Zeeman field B, exchange coupled to the spin $\mathbf{s}=\frac{1}{2}c_1^\dagger\boldsymbol{\sigma}c_1$ of the first site of a chain of length N of fermions with spin μ and exponentially decreasing hopping matrix elements along the chain ($\xi_n\sim\Lambda^{-n/2}$). $\mathcal{H}^N$ lives on a Hilbert space spanned by the set of $d_I d^N$ basis states $\{|i_0,i_1,i_2,\ldots i_N\rangle\}$, where i_0 labels the d_I possible impurity states and i_n (for $n=1,\ldots,N$) the d possible

states of site n (for the Kondo model, $i_0=\{\uparrow,\downarrow\}$ and for all other sites $i_n=\{0,\uparrow,\downarrow,\uparrow\downarrow\}$, i.e., $d_I=2$ and $d=4$).

To diagonalize the model, NRG starts with a chain of length $(\bar{n}-1)$, chosen sufficiently small that $\mathcal{H}^{\bar{n}-1}$ can be diagonalized exactly, yielding a set of eigenstates $|\psi_\alpha^{\bar{n}-1}\rangle$. One continues with the subsequent iterative prescription: project $\mathcal{H}^{\bar{n}-1}$ onto the subspace spanned by its lowest D eigenstates, where $D<d_I d^{\bar{n}-1}$ is a control parameter (typically between 500 and 2000); add site $\bar{n}$ to the chain and diagonalize $\mathcal{H}^{\bar{n}}$ in the enlarged (Dd)-dimensional Hilbert space, writing the eigenstates as

$$|\psi_\beta^{\bar{n}}\rangle = \sum_{i_{\bar{n}}=1}^{d}\sum_{\alpha=1}^{D} |\psi_\alpha^{\bar{n}-1}\rangle|i_{\bar{n}}\rangle P_{\alpha\beta}^{[i_{\bar{n}}]}, \tag{2}$$

where the coefficients have been arranged in a matrix $P_{\alpha\beta}^{[i_{\bar{n}}]}$ with matrix indices α, β, labeled by the site index $\bar{n}$, and state index $i_{\bar{n}}$; rescale the eigenenergies by a factor $\Lambda^{1/2}$; and repeat, until the eigenspectrum converges, typically for chain lengths N of order 40 to 60. At each step of the iteration, the eigenstates of $\mathcal{H}^N$ can thus be written [by repeated use of Eq. (2)] in the form of a so-called matrix-product-state,

$$|\psi_\alpha^N\rangle = P_{\alpha_0}^{[i_0]} P_{\alpha_0\alpha_1}^{[i_1]} P_{\alpha_1\alpha_2}^{[i_2]} \cdots P_{\alpha_{N-1}\alpha}^{[i_N]} |i_0, i_1, \ldots, i_N\rangle \tag{3}$$

(summation over repeated indices implied). The ground state is then the lowest eigenstate of the effective Hamiltonian $\mathcal{H}_{\alpha\beta}^N=\langle\psi_\alpha^N|\mathcal{H}^N|\psi_\beta^N\rangle$, i.e., the projection of the original $\mathcal{H}$ on the subspace of MPS of the form (3).

II. VMPS OPTIMIZATION

Let us now be more ambitious and aim to find the *best possible* description of the ground state within the space of all MPSs of the form (3), using the matrix elements of the matrices $\{P^{[n]}\}$ with $P^{[n]}\equiv\{P^{[i_n]}\}$ as *variational parameters* to minimize the energy. Using a Lagrange multiplier to ensure normalization, we thus study the following optimization problem:

$$\min_{|\psi^N\rangle\in\{\mathrm{MPS}\}} [\langle\psi^N|\mathcal{H}^N|\psi^N\rangle - \lambda\langle\psi^N|\psi^N\rangle]. \tag{4}$$

This cost function is multiquadratic in the $d_I+d(N-1)$ matrices $\{P^{[n]}\}$ with a multiquadratic constraint. Such problems can be solved efficiently using an iterative method in which one fixes all but one (let's say the $\bar{n}$'th) of the matrices $\{P^{[n]}\}$ at each step; the optimal $P^{[\bar{n}]}$ minimizing the cost function given the fixed values of the other matrices can then be found by solving an eigenvalue problem.[8] With $P^{[n]}$ optimized, one proceeds the same way with $P^{[\bar{n}+1]}$ and so on. When all matrices have been optimized locally, one sweeps back again, and so forth. By construction, the method is guaranteed to converge as the energy goes down at every step of the iteration, having the ground-state energy as a global lower bound. Given the rather monotonic hopping amplitudes, we did not encounter problems with local minima.

In contrast, NRG constructs the ground state in a single *one-way* sweep along the chain: each $P^{[n]}$ is thus calculated only once, without allowing for possible feedback of P's calculated later. Yet viewed in the above context, the ground-state energy can be lowered further by MPS optimization sweeps. This accounts for the *feedback* of information from low-to-high-energy scales. This feedback may be small in practice, but it is not strictly zero, and its importance increases as the logarithmic discretization is refined by taking $\Lambda\to 1$. Note that the computational complexity of both VMPS optimization and NRG scales as NdD^3,[8,9] and symmetries can be exploited (with similar effort) in both approaches. The inclusion of feedback leads to a better description of spectral features at high frequencies, which are of importance in out-of-equilibrium and time-dependent impurity problems. Moreover, it also allows to relax the logarithmic discretization scheme, further improving the description of structures at high frequency as illustrated below.

The result of a converged set of optimization sweeps is a VMPS ground state $|\tilde{\psi}_0^N\rangle$ of the form (3); exploiting a gauge degree of freedom,[8] the $\tilde{P}$'s occurring therein can always be chosen such that all vectors $|\tilde{\psi}_\alpha^n\rangle=[\tilde{P}^{[i_0]}\ldots\tilde{P}^{[i_n]}]_\alpha|i_0,\ldots,i_n\rangle$ are orthonormal. The effective Hamiltonian at chain length n, the central object in NRG, is then $\tilde{\mathcal{H}}_{\alpha\beta}^n=\langle\tilde{\psi}_\alpha^n|\Lambda^{n/2}\mathcal{H}^n|\tilde{\psi}_\beta^n\rangle$. Its eigenspectrum can be monitored as n increases, resulting in an energy level flow along the chain.

III. GREEN'S FUNCTIONS

Similar techniques also allow Green's functions to be calculated variationally.[15] The typical Green's functions of interest are of the form $G_\eta^c(\omega)=\langle\psi_0|c|\chi\rangle$ where $|\chi\rangle$, commonly called a correction vector,[16] is defined by

$$|\chi\rangle \equiv \frac{1}{\omega-\mathcal{H}+i\eta}c^\dagger|\psi_0\rangle, \tag{5}$$

with $|\psi_0\rangle$ the ground state of the system, e.g. calculated using the VMPS approach and thus represented as MPS. The spectral density is then given by $\mathcal{A}(\omega)=-\lim_{\eta\to 0}\frac{1}{\pi}\Im\mathrm{m}(G_\eta^c(\omega))$. The (unnormalized) state $|\chi\rangle$ may be calculated *variationally* within the set of MPS by optimizing the weighted norm

$$\mathcal{N}=\left\|\chi> - \frac{1}{\mathcal{H}-\omega-i\eta}c^\dagger|\psi_0\rangle\right\|_{W=(\mathcal{H}-\omega)^2+\eta^2}, \tag{6}$$

where $\|\xi>\|_W^2\equiv\langle\xi|W|\xi\rangle$, and weight $W>0$ such that it yields a quadratic equation. Writing $|\chi\rangle\equiv|\chi_r\rangle+i|\chi_i\rangle$ and assuming $\mathcal{H}$, $|\psi_0\rangle$, $|\chi_r\rangle\equiv\Re\mathrm{e}|\chi\rangle$, and $|\chi_i\rangle\equiv\Im\mathrm{m}|\chi\rangle$ real, this norm can be written as (compare Ref. 14) $\mathcal{N}^2=\langle\chi_r|(\mathcal{H}-\omega)^2+\eta^2|\chi_r\rangle - 2\langle\chi_r|(\mathcal{H}-\omega)c^\dagger|\psi_0\rangle+\langle\chi_i|(\mathcal{H}-\omega)^2+\eta^2|\chi_i\rangle-2\eta\langle\chi_i|c^\dagger|\psi_0\rangle + \langle\psi_0|cc^\dagger|\psi_0\rangle$. Minimizing $\mathcal{N}$ efficiently by optimizing one P at a time leads to two independent optimizations over $|\chi_r\rangle$ and $|\chi_i\rangle$, respectively. Both involve only multilinear terms such that each iteration step requires to solve a sparse linear set of equations.[10]

Minimizing $\mathcal{N}$ involves the calculation of $\mathcal{H}^2$, which can be done efficiently as follows. Generally speaking, $\mathcal{H}$ has the structure of a spin chain with only nearest-neighbor couplings as shown in Eq. (1). Naively one expects that one will have to evaluate on the order of N^2 expectation values of

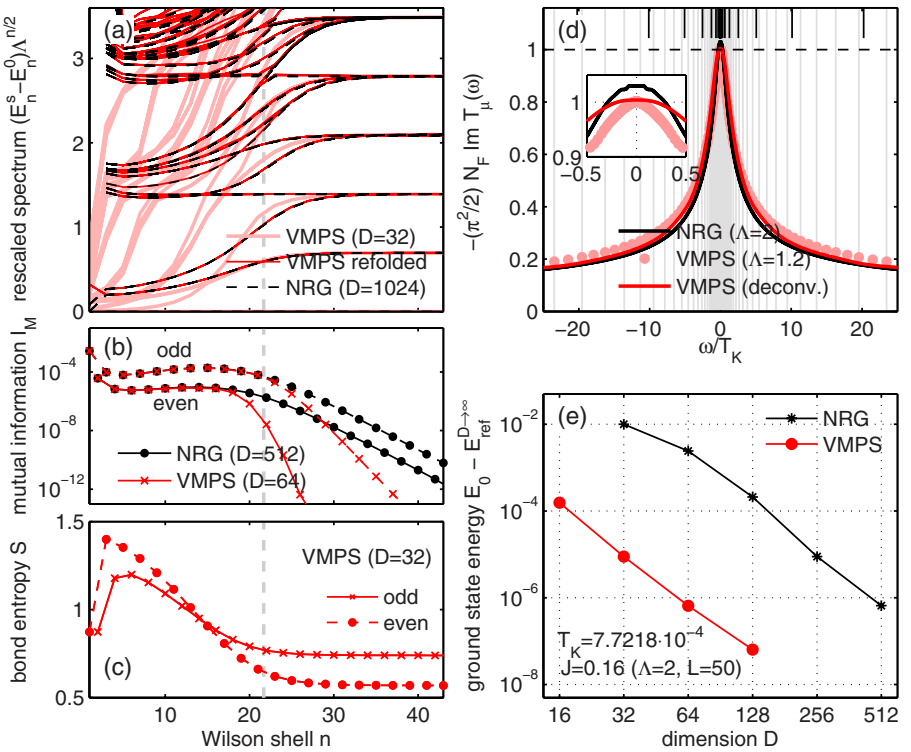

FIG. 1. (Color online) Comparison of VMPS and NRG data for logarithmic discretization of the Kondo model as in Eq. (1) for $J=0.16$ and $\Lambda=2$ if not specified otherwise. (a) Energy level flow of the Kondo model as a function of site index n obtained from $\mathcal{H}_\mu^{\mathrm{eff}}$ of a variationally optimized MPS with $D_{\mathrm{MPS}}=32$ (light red/light solid), of the corresponding recombined spin chains (red/dark solid) (Ref. 17), and from NRG using $D_{\mathrm{NRG}}=32^2$ states (dashed black). The Wilson shell corresponding to $T_K \equiv \sqrt{J}e^{-1/J}$ is indicated by the vertical dashed line through panels (a) to (c). (b) Correlation along the Wilson chain between spin up and spin down at site n in terms of mutual information $I_M(n) \equiv S(n_\uparrow)+S(n_\downarrow)-S(n_\uparrow,n_\downarrow)$. Here S is the entropy of the reduced density matrix of the groundstate with respect to the indicated subspace (Ref. 17) (solid for even, dashed for odd sites n). (c) Bond entropy S along the unfolded Wilson chain, where S is the usual von Neumann entropy of the VMPS reduced density matrix when going from site n to $n+1$, plotted for even and odd iterations, respectively. (d) Comparison of T matrix ($\Im m T_\mu$, see also Fig. 2) for $B=0$ between VMPS and NRG, including deconvoluted VMPS data (see Appendix). Inset shows zoom into peak at $\omega=0$. The significantly smaller $\Lambda=1.2$ applicable for VMPS (discretization intervals are indicated by vertical lines) shows clearly improved agreement with the Friedel sum rule $T(0)\pi^2/2=1$. (e) Comparison of ground-state energy of the Kondo Hamiltonian Eq. (1) for fixed chain length relative to the extrapolated energy for $D\to\infty$ for VMPS and NRG as function of the dimension D of states kept.

local observables. There is, however, a clever linear scheme that only requires iterative update of a set of effective operators. Therefore the computational complexity of calculating ϵ scales as ND^3 similar to just evaluating the energy $\langle\psi|\mathcal{H}|\psi\rangle$. As a side product, this leads to efficient algorithms for calculating excited eigenstates of Hamiltonians close to a fixed energy E by minimizing $\langle\psi|(\mathcal{H}-E)^2|\psi\rangle$. Moreover, it can be used to estimate errors on eigenenergies as it can be shown that there exists an exact eigenvalue E_{ex} within an interval around E specified by $\epsilon=\sqrt{\langle\psi|(\mathcal{H}-E)^2|\psi\rangle}$.

For quantum impurity systems with sharp features such as the Kondo model discussed below, it should be noted, however, that the broadening η may have to be chosen extremely small. In this case, the minimization of $\mathcal{N}$ in Eq. (6) can become increasingly ill conditioned as $\eta\to 0$ (see Appendix), with conditioning deteriorating quadratically in η. If one directly solves $\delta/\delta\langle P^{[n]}|[\langle\chi|(\mathcal{H}-\omega-i\eta)|\chi\rangle-\langle\chi|c^\dagger|\psi\rangle]\equiv 0$ by a nonhermitian equation solver such as the biconjugate gradient method, conditioning deteriorates only linearly. This is the strategy that has been followed to obtain the results reported below.

IV. APPLICATION TO KONDO MODEL

Let us now illustrate above strategies by applying them to the Kondo model. Since the Hamiltonian in Eq. (1) couples ↑ and ↓ band electrons only via the impurity spin, it is possible (see also Refs. 5 and 17) to "unfold" the semi-infinite Wilson chain into an infinite one, with ↑ band states to the left of the impurity and ↓ states to the right, and hopping amplitudes decreasing in both directions as $\Lambda^{-|n|/2}$. Since the left and right end regions of the chain, which describe the model's low-energy properties, are far apart and hence interact only weakly with each other [analyzed quantitatively in terms of mutual information in Fig. 1(b)], the effective Hamiltonian for these low energies will be of the form $\mathcal{H}_\uparrow^{\mathrm{eff}}\otimes 11_\downarrow + 11_\uparrow \otimes \mathcal{H}_\downarrow^{\mathrm{eff}}$. Due to the symmetry of the Kondo coupling, $\mathcal{H}_\uparrow^{\mathrm{eff}}$ and $\mathcal{H}_\downarrow^{\mathrm{eff}}$ have the same eigenspectrum for $n\gg 1$, such that the fixed point spectrum is already well reflected by analyzing either one, as illustrated in Fig. 1(a). Note that for a direct comparison with NRG, the spin chains can be *recombined* within VMPS.[17] The resulting standard energy flow diagram presented in panel (a) for VMPS and NRG, respectively,

show excellent agreement for low energies for all n including the fixed point spectrum.

In addition to the energy flow diagram in panel (a), convergence with and hence sensitivity on the Kondo energy scale is also nicely seen in other quantities typically calculated within VMPS: in the internal entanglement of the Wilson chain as function of site n in terms of mutual information, shown in panel (b), and the entanglement of Wilson chain up to site n with the remainder of the Wilson chain, shown in panel (c). Note that due to intrinsic even/odd effects of the model, the data from even/odd Wilson sites is plotted separately.

The dimensions of the effective Hilbert spaces needed for VMPS for the unfolded Wilson chain and NRG for the inevitably folded chain to capture the low-energy properties (here energy resolution better than T_K) are roughly related by $D_{\mathrm{MPS}} \sim \sqrt{D_{\mathrm{NRG}}}$,[17] implying significant computational gain with VMPS, as calculation time scales as D^3 for both. Indeed, Fig. 1(e) shows that VMPS has three orders of magnitude of better precision for the *same* D. More generally, if the impurity couples to n electronic bands (channels), the Wilson chain may be unfolded into a starlike structure of $2n$ branches, with $D_{\mathrm{MPS}} \sim D_{\mathrm{NRG}}^{1/2n}$. This implies that for maintaining a desired precision in going from 1 to n channels, D_{MPS} will stay roughly constant, and calculation time for all sites other than the impurity will scale merely *linearly* with the number of channels. Whether the chains can be unfolded in practice can easily be established by checking whether or not the correlation between them, characterized, e.g., in terms of mutual information, decays rapidly with increasing n [cf. Fig. 1(b) and caption].

V. ADAPTIVE DISCRETIZATION

Through its variational character, VMPS does not rely on logarithmic discretization crucial for NRG. The potential of greatly enhanced energy resolution using VMPS is already indicated by the $\Lambda=1.2$ data in Fig. 1(d). It is illustrated to full extent in Fig. 2, showing the splitting of the Kondo peak in the presence of a strong magnetic field calculated using VMPS (bare: dots, deconvoluted: red solid), standard NRG (blue dashed), and perturbatively[18] (black).

To obtain the VMPS results of Fig. 2, we used an *adapted* discretization scheme for the energies ε_k of the conduction band Hamiltonian $H_{\mathrm{band}}=\Sigma_{k\mu}\varepsilon_k c_{k\mu}^\dagger c_{k\mu}$ that forms the starting point for deriving the Wilson chain like Hamiltonian of Eq. (1).[1] Namely, we use a linear or logarithmic discretization scheme for $|\varepsilon_k|<B$ or $>B$, respectively, (as illustrated by light vertical lines in Fig. 2). The nearest-neighbor coupling amplitudes ξ_n of the resulting, modified Wilson chain decay only very slowly with n once the energy scale of site n, namely, $\Lambda^{-n/2}$, drops below B, in contrast to their usual exponential decay for a standard Wilson chain (see inset of Fig. 2, VMPS vs $\Lambda=1.7$ NRG coupling). The slow decay of ξ_n implies an increased energy resolution at energies up to B, at the cost of a loss of energy scale separation. While the latter fact implies that NRG cannot be used on such a chain, the VMPS approach does not suffer from this limitation. Indeed, it exploits the enhanced energy resolution at energies of order B to yield spectral peaks around $\omega \simeq B$ that are significantly sharper than those obtainable by NRG (Fig. 2, compare dotted data points to dashed line). The resolution can be enhanced even further (Fig. 2, solid thick light line) by applying a deconvolution scheme to the VMPS data, detailed in the appendix, to account for the broadening effects of using an *a priori* finite η required within the VMPS approach.

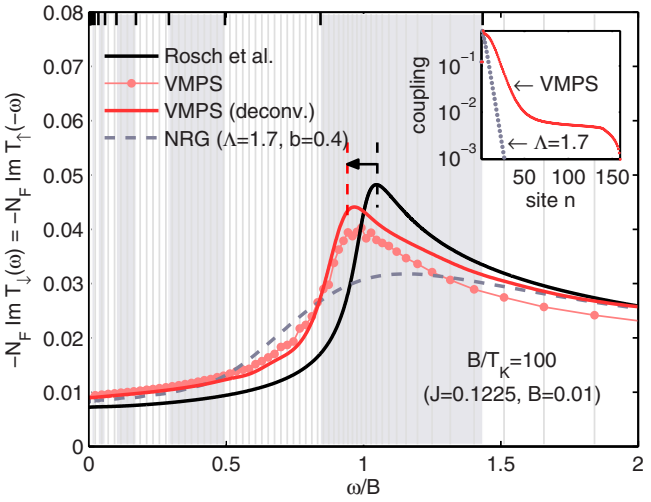

FIG. 2. (Color online) Impurity spectral function for the Kondo model $-N_F \Im \mathrm{m} T_\mu(\omega)=J^2\langle\langle \mathcal{O}_\mu^\dagger | \mathcal{O}_\mu\rangle\rangle_\omega$ for $B \gg T_K$, where $\mathcal{O}_\mu \equiv \mathbf{S}\cdot\boldsymbol{\sigma}_{\mu\mu'}c_{\mu'}^\dagger$ and N_F is the density of states at the Fermi energy, calculated with VMPS (dots: raw data, red solid: deconvoluted), NRG (dashed), and perturbative (black solid) (Ref. 18). For NRG, $D=1024$ states were kept, using a log-Gauss broadening parameter (Ref. 19) of $b=0.4$. According to Ref. 18, the peak of the perturbative result should be shifted in ω by $B/2\,\log(B/T_K)$ (arrow). NRG and VMPS discretization intervals are indicated by shaded areas and gray vertical lines, respectively. Due to the increased linear resolution for $|\omega| \leq B$, the number of states retained within VMPS needed to be increased, and was dynamically governed by either a threshold of $4\cdot 10^{-8}$ in discarded weight or a maximum number of states of $D=512$. The latter was required only for frequencies around $\omega \sim B$. The inset shows the hopping amplitudes corresponding to standard logarithmic ($\Lambda=1.7$) and adapted (VMPS) discretization schemes. The required Lorentzian broadening η of the VMPS data smears out sharper features. Deconvolution (targeting with adaptive spline) together with subsequent GAUSSIAN broadening was applied to obtain the solid light line (see Appendix).

Note that such a resolution is out of reach for conventional NRG, whose discretization intervals (shaded intervals), even for comparatively small choice of $\Lambda=1.7$, are much broader than the spectral features of interest. Note that the NRG data shown here is, by conventional NRG standards, of high quality: first, we used a rather small value of $\Lambda=1.7$, implying high-energy resolution, by NRG standards; second, we employed the recently developed full density-matrix (FDM) approach,[19,20] which incorporates systematic improvements relative to previous NRG implementations. We have tried extensively to improve the quality of our NRG data via z-averaging,[21] but have found this to be of limited use.

The line shape of our deconvoluted data (red solid line) agrees well with the analytic RG calculation[18] (black solid

line), perturbative in $1/\log(B/T_K)$. The peak positions agree well also after a shift in ω by $-B/2\log(B/T_K)$ of the perturbative result suggested by[18] is taken into account.

As pointed out in the context of Fig. 1, numerical resources in terms of matrix dimensions can be drastically reduced within VMPS when applied to the NRG discretized model, in that the variational freedom provides a highly adaptive method. However, this does come at a price. While the calculation of spectral functions within NRG for the full frequency range are obtained in a single run about as expensive numerically as the iterative diagonalization of the NRG Hamiltonian and as such highly efficient, the correction vector method [cf. Eq. (5)] provides an optimal setting for one frequency at a time. This is highly tailored toward analyzing certain features in frequency space, but implies that for every spectral data point a new correction vector must be obtained, which is itself equally expensive numerically as the calculation of the ground state. Nevertheless, in situations that become computationally hard in NRG or are simply out of reach for NRG due to the required rather crude coarse graining of the conduction band, VMPS does provide a well-controlled technique that can clearly compete and in certain cases outperform NRG. In the example given in Fig. 2, the logarithmic discretization scheme was adapted by introducing an energy interval from $-B$ to B in which the level spacing was chosen to be essentially uniform. It appears, indeed, that for describing dynamical features at frequencies $\omega \sim B$, *all* states with frequencies $|\omega| \leq B$ are equally important, which necessitates the use of a uniform level spacing from $-B$ to B. Of course, this does break energy scale separation from the very outset.

VI. OUTLOOK

Let us finish by pointing out that the MPS approach can readily be extended to the case of finite temperatures by using matrix-product density operators[10] instead of MPS, and to time-dependent problems [such as $\mathcal{H}=\mathcal{H}(t)$ or nonequilibrium initial conditions], by using the recently developed adaptive time-dependent DMRG[11] and MPS analogs thereof.[10] Exploratory work in this direction has been very encouraging.[22]

In conclusion, the MPS approach provides a natural language for simulating quantum impurity models. The underlying reason is that these models, when formulated on the Wilson chain, feature only nearest-neighbor interactions. Their low-energy states are thus determined mainly by their nearest-neighbor reduced density matrices, for which very good approximations can be obtained by suitably optimizing the set of matrices constituting a MPS.[23] We also showed how these could be used for a direct (quasi) variational evaluation of Green's functions.

Recently, it has come to our attention that two recent papers by Freyn and Florens[24] and Zitko and Pruschke[25] who claimed improved resolution of NRG spectral functions. Besides properly accounting for the wave function renormalization A_Λ due to discretization,[26] Ref. 25 is heavily based on z-averaging[21] with modest success for finite frequencies—see for example Fig. 8 in Ref. 25 which shows spurious oscillations. It is exactly these spurious oscillations we had also seen in the z-averaging done excessively for our model. In order to get rid of these spurious oscillations in a systematic unbiased manner, however, one would have to rebroaden the data to get discretization-independent correlation function. Hence, although z-averaging does show modest improvements (as known since Ref. 21), it cannot be expected to cure in much detail the rather crude coarse graining of the conduction band put into the model from the beginning. Reference 24 introduced a procedure for broadening the raw NRG data to obtain smooth spectral peaks, employing a frequency-dependent broadening parameter $b(\omega)$. This led to significantly increased resolution for spectral peaks of the spin-boson model with very weak damping. However, when we tried this method for the present Kondo model, the improvements over conventional NRG broadening techniques were also found to be rather modest.

ACKNOWLEDGMENTS

We gratefully acknowledge fruitful discussions with M. Sindel, W. Hofstetter, G. Uhrig, and F. Anders. This work was supported by DFG (SFB 631, SFB-TR 12, De 730/3-1, De 730/3-2), FWF (SFB FoQuS), GIF (I-857), European projects (Spintronics RTN, SCALA, QUEVADIS, QUERG), Kompetenznetzwerk der Bayerischen Staatsregierung Quanteninformation, the Gordon and Betty Moore Foundation (Information Science and Technology Initiative, Caltech), and in part by the National Science Foundation under Grant No. NSF PHY05-51164. Financial support of the Excellence Cluster Nanosystems Initiative Munich (NIM) is gratefully acknowledged.

APPENDIX: DECONVOLUTION OF SPECTRAL DATA

DMRG obtains spectral data from a discretized model Hamiltonian. In order for the spectral data to be smooth, an intrinsic frequency-dependent Lorentzian broadening η is applied during the calculation of the correction vector $|\chi\rangle_k$ at frequency ω_k [cf. Eq. (5)],

$$\delta_{\eta_k}(\omega-\omega_k) \equiv \frac{\eta_k}{\pi}\frac{1}{(\omega-\omega_k)^2+\eta_k^2}. \tag{7}$$

Since the original model has a continuous spectrum, the broadening η_k should be chosen of the order or larger than the artificial coarse grained discretization intervals δ_ω. Larger η of course improves numerical convergence. However, since Lorentzian broadening produces longer tails than for example GAUSSIAN broadening, this makes it more susceptible to pronounced spectral features close by. Our general strategy for more efficient numerical treatment was then as follows. (i) Choose somewhat larger $\eta(\eta \simeq 2\delta_\omega)$ throughout the calculation. (ii) Deconvolve the raw data to such an extent that the underlying discrete structure already becomes visible again, (iii) followed by a GAUSSIAN smoothening procedure which then acts more locally. Let us describe step (ii) in more detail.

Broadening, by construction, *looses* information. Hence trying to obtain the original data from the broadened data via deconvolution is intrinsically ill conditioned. In literature there are several ways of dealing with this problem, most prominently maximum entropy algorithms (see Refs. 5 and 27). Our approach is targeting the actual spectral function using the knowledge about the Lorentzian broadening used during the VMPS calculation, combined with adaptive spline. Given the data $\tilde{A}(\omega)$ obtained through VMPS, let us propose the existence of some smooth but *a priori* unknown target curve $A(\omega)$, which when broadened the *same* way as the VMPS data using exactly the same η_k via a Lorenzian broadening kernel

$$\tilde{A}_k \equiv \tilde{A}(\omega_k) = \int_{-\infty}^{\infty} d\omega' A(\omega') \delta_{\eta_k}(\omega' - \omega_k), \tag{8}$$

reproduces the original data $\tilde{A}(\omega)$. Direct inversion of above equation as it is ill conditioned, as already mentioned, and not useful in practice.

Let us assume the unknown target curve $A(\omega)$ is smooth and parametrized by piecewise polynomials. Given the data points ω_k with $k=1\ldots N$, the intervals in between these values will be approximated in the spirit of adaptive spline functions[27] by 3rd order polynomials ($k=1\ldots N-1$)

$$f_k(\omega) \equiv \begin{cases} a_k + b_k(\omega-\omega_k) + c_k(\omega-\omega_k)^2 + d_k(\omega-\omega_k)^3 & \text{for } \omega \in [\omega_k, \omega_{k+1}] \\ 0 & \text{otherwise.} \end{cases} \tag{9}$$

Since spectral functions decay as $1/\omega^2$ for large ω, for our purposes the ends are extrapolated asymptotically to infinity, allowing both $1/\omega$ and $1/\omega^2$ polynomials

$$f_0(\omega) \equiv \begin{cases} \dfrac{a_0}{\omega} + \dfrac{b_0}{\omega^2} & \omega \le \omega_1 \\ 0 & \text{otherwise} \end{cases}$$

$$f_N(\omega) \equiv \begin{cases} \dfrac{a_N}{\omega} + \dfrac{b_N}{\omega^2} & \omega \ge \omega_N \\ 0 & \text{otherwise.} \end{cases} \tag{10}$$

In total, this results in $4(N-1)+2\times 2=4N$ parameters, with the target function parametrized piecewise as $A(\omega)\equiv f(\omega) \equiv \Sigma_{k=0}^{N} f_k(\omega)$. In cases where one has not approached the asymptotic limit yet, the ends may simply be modeled also by Eq. (9), taking $c_0=d_0=c_N=d_N=0$. Moreover, if information about the gradient $f'(\omega)$ is known, it can be built in straightforwardly in the present scheme by replacing b_k.

The parameters for the piecewise parametrization are solved for by requiring the following set of conditions:

(i) The function f should be continuous and smooth by requiring that f, f', and f'' are continuous ($3N$ equations).

(ii) The function f, when broadened as in Eq. (8), should reproduce the VMPS data $\tilde{A}_k$

$$\tilde{A}_k^c \equiv \sum_{k'=0}^{N} \int_{\omega_{k'}}^{\omega_{k'+1}} d\omega' f_{k'}(\omega') \frac{\eta_k/\pi}{(\omega'-\omega_k)^2+\eta_k^2} \tag{11}$$

$$\tilde{A}_k - \tilde{A}_k^c = p_k r_k \tag{12}$$

where $r_k \equiv f_k^{(3)}(\omega_k) - f_{k-1}^{(3)}(\omega_k)$ and $\omega_0 \equiv -\infty$, $\omega_{N+1} \equiv +\infty$ (N equations).

In the spirit of adaptive spline, the third derivative of the piecewise polynomials is no longer required to be continuous. Its jump r_k is set proportional to the change in $\tilde{A}_k - \tilde{A}_k^c$ introducing the additional prespecified parameter set p_k, kept small for our purposes (note that enforcing the strict equality $\tilde{A}_k^c = \tilde{A}_k$ by setting $p_k=0$ would result in an ill-conditioned problem).

If interval spacings specified by ω_k are nonuniform, the p_k have to be adapted accordingly. For this paper we used $p_k = p\cdot(\omega_{k+1}-\omega_k)^\alpha$ with p on the order of 10^{-6} and $\alpha \simeq 1$. With p_k fixed, Eqs. (11) and (12) determine all spline parameters uniquely in terms of the original VMPS data $\tilde{A}_k$. The integrals emerging out of Eq. (11) can all be evaluated analytically. The final inversion of Eq. (11) to obtain the parameters for $f(\omega)$ is well behaved for small but finite p, small enough to clearly sharpen spectral features.

[1] K. G. Wilson, Rev. Mod. Phys. **47**, 773 (1975).
[2] H. R. Krishna-murthy, J. W. Wilkins, and K. G. Wilson, Phys. Rev. B **21**, 1003 (1980).
[3] T. A. Costi, A. C. Hewson, and V. Zlatic, J. Phys.: Condens. Matter **6**, 2519 (1994).
[4] W. Hofstetter, Phys. Rev. Lett. **85**, 1508 (2000).
[5] C. Raas, G. S. Uhrig and F. B. Anders, Phys. Rev. B **69**, 041102(R) (2004); C. Raas and G. S. Uhrig, Eur. Phys. J. B **45**, 293 (2005).
[6] R. Bulla, A. C. Hewson, and Th. Pruschke, J. Phys.: Condens. Matter **10**, 8365 (1998); R. Bulla, N. H. Tong, and M. Vojta, Phys. Rev. Lett. **91**, 170601 (2003).

[7] M. Fannes, B. Nachtergaele, and R. F. Werner, Commun. Math. Phys. **144**, 443 (1992); S. Ostlund and S. Rommer, Phys. Rev. Lett. **75**, 3537 (1995); J. Dukelsky, M. A. Martín-Delgado, T. Nishino, and G. Sierra, Europhys. Lett. **43**, 457 (1998); H. Takasaki, Toshiya Hikihara, and Tomotoshi NishinoJ. Phys. Soc. Jpn. **68**, 1537 (1999).

[8] F. Verstraete, D. Porras, and J. I. Cirac, Phys. Rev. Lett. **93**, 227205 (2004).

[9] S. R. White, Phys. Rev. Lett. **69**, 2863 (1992); U. Schollwöck, Rev. Mod. Phys. **77**, 259 (2005).

[10] F. Verstraete, J.-J. García-Ripoll, and J. I. Cirac, Phys. Rev. Lett. **93**, 207204 (2004).

[11] G. Vidal, Phys. Rev. Lett. **93**, 040502 (2004); A. J. Daley, C. Kollath, U. Schollwöck, and G. Vidal, J. Stat. Mech. Theor. Exp. (2004) P04005; S. R. White and A. E. Feiguin, Phys. Rev. Lett. **93**, 076401 (2004).

[12] K. A. Hallberg, Phys. Rev. B **52**, R9827 (1995).

[13] T. D. Kühner and S. R. White, Phys. Rev. B **60**, 335 (1999).

[14] E. Jeckelmann, Phys. Rev. B **66**, 045114 (2002).

[15] Compared to other techniques for calculating Green's functions (Refs. 3–5, 12–14, and 28), the VMPS approach proposed here has the advantage that it is variational, and hence in principle optimal within the set of MPS. It is more efficient than the continued fraction method (Ref. 12), the correction vector method (Ref. 13) and dynamical DMRG (Ref. 14), because each of these methods require several states to be calculated simultaneously, thus requiring larger D for the same precision.

[16] Z. G. Soos and S. Ramasesha, J. Chem. Phys. **90**, 1067 (1989).

[17] H. Saberi, A. Weichselbaum, and J. von Delft, Phys. Rev. B **78**, 035124 (2008).

[18] A. Rosch, T. A. Costi, J. Paaske, and P. Wolfle, Phys. Rev. B **68**, 014430 (2003); M. Garst, P. Wolfle, L. Borda, J. von Delft, and L. Glazman, *ibid.* **72**, 205125 (2005).

[19] A. Weichselbaum and J. von Delft, Phys. Rev. Lett. **99**, 076402 (2007).

[20] R. Peters, T. Pruschke, and F. B. Anders, Phys. Rev. B **74**, 245114 (2006).

[21] M. Yoshida, M. A. Whitaker, and L. N. Oliveira, Phys. Rev. B **41**, 9403 (1990).

[22] C. Guo, A. Weichselbaum, S. Kehrein, T. Xiang, and J. von Delft, Phys. Rev. B **79**, 115137 (2009).

[23] F. Verstraete and J. I. Cirac, Phys. Rev. B **73**, 094423 (2006).

[24] A. Freyn and S. Florens, Phys. Rev. B **79**, 121102(R) (2009).

[25] R. Zitko and T. Pruschke, Phys. Rev. B **79**, 085106 (2009).

[26] V. L. Campo and L. N. Oliveira, Phys. Rev. B **72**, 104432 (2005).

[27] W. H. Press, S. A. Teukolsky, W. T. Vetterling, and B. P. Flannery, *Numerical Recipies in C*, 2nd ed. (Cambridge University Press, Cambridge, 1993).

[28] S. Nishimoto and E. Jeckelmann, J. Phys.: Condens. Matter **16**, 613 (2004).